Contents lists available at Egyptian Knowledge Bank

Labyrinth: Fayoum Journal of Science and Interdisciplinary Studies

Journal homepage: https://lfjsis.journals.ekb.eg/

Exploring the metal tungstate oxides (MWO_4; M = Ca, Sr, Ba, and Pb) as radiation shielding materials: a simulation study

Said M. Kassem [a,b,*], Adel M. El Sayed [a], S. Ebraheem [b], A. I. Helal [c], Y. Y. Ebaid [a]

[a] Physics Department, Faculty of Science, Fayoum University, El Fayoum 63514, Egypt.

[b] Radiation Protection and Dosimetry Department, National Center for Radiation Research and Technology (NCRRT), Egyptian Atomic Energy Authority (EAEA), Cairo, Egypt.

[c] Experimental Nuclear Physics Department, Nuclear Research Center (NRC), Egyptian Atomic Energy Authority (EAEA), Cairo, Egypt.

A R T I C L E I N F O

Keywords:

Metal tungstate oxides
MCNP
Radiation shielding performances
Phy-X/PSD

A B S T R A C T

Environmentally hazardous radiation sources can negatively affect human health. For example, tumors, cancer, a decrease in lymphocyte cell count, and severe cases of fatalities. Because of this, the present work aims to explore the radiation-protecting performances of the metal-tungstate oxides: $CaWO_4$, $SrWO_4$, $BaWO_4$, and $PbWO_4$ as a comparative study that provides effective strategy for developing sustainable and alternative shield material. The mean track length of incoming photons inside four distinct metal tungstate oxides has been determined using the Monte Carlo simulation code. Then, other significant gamma-ray shielding characteristics were computed based on the predicted track length. For all samples, attenuation coefficients are estimated by MCNP5 simulation code, which showed satisfactory agreement with the Phy-X/PSD results. It also used to figure out the half-value layer, mean free path, effective atomic number, and effective electron density. The mass attenuation coefficient and effective atomic number are energy and density dependency, have maximum values at the lowest energies and minimum values at the highest energies. The study findings imply that the atomic density and metal tungstate oxide composition of the material determine the correlation between the photon and the shield material. The results showed that the maximum mass attenuation coefficient was achieved for $PbWO_4$ that is a superior candidate for radiation shielding applications.

1. Introduction

Since ionizing radiation is used so often in the medical field, the military, and numerous other businesses, the problem is presently growing worse. It is significant that ionizing radiation may cause harm to human health. Many studies on radiation-protective materials have been conducted in an effort to address these shortcomings [1-3]. Lead, however, is a highly dangerous material for both people and their surroundings. Due to its large atomic number Z (82), higher density (11.29 g/cm^3), and inexpensive cost, lead is frequently employed in radiation shields [2]. As a result, it is necessary to identify and create substitutes that provide equally effective radiation protection. In the last few years, a wide range of compositions have been suggested and investigated for radiation shielding [3].

Structure of a perovskite with the general chemical formula ABX_4. The X atoms (usually oxygen), the B atoms (a smaller metal cation, such as W, V, Mn, etc.), and the A atoms (a larger metal cation, such as Ca, Ba, Fe, Sr, Pb, La, etc.) [4-6]. Among those materials, the metal tungstate based on the perovskite-structured ABO_4 might be capable of radiation protection. Among the well-known metal tungstate oxides ABO_4 perovskites form, $PbWO_4$ and $BaWO_4$ exhibit remarkable multifunctional properties [4]. In addition to being non-organic in structure, metal tungstate oxides are hard, less porous, long-lasting, and environmentally friendly [7-12].

To enhance the polymer composite's radiation shielding capabilities, for example, $Bi_2(WO_4)_3$ was reinforced into the polyester composite has been recently reported. The metal tungstate oxides have better performance in radiation protecting [13]. An investigation of metal composites series based on tungsten (Bi_2WO_6, $PbWO_4$, and $Pb_{0.82}Bi_{0.12}WO_4/W_{0.5}Pb_{0.5}Bi_{12}O_{20}$) has been studied as effective protective blocks against gamma radiation [14]. Also evaluate the validity of LDPE/SBR polymer bland with 5, 10, 15, and 20 wt.% of $BaWO_4/B_2O_3$ nanofillers against radiation [15]. The radiation shielding parameters of $BaWO_4$ metal tungstate oxides doped with Ho_2O_3 oxides have been assessed using the MCNP code for gamma rays [16]. Very recently,

* Corresponding author.
E-mail address: saidmoawad2@gmail.com (Said M. Kassem); Tel.: +201091878513

DOI: 10.21608/IFJSIS.2024.273401.1067
Received 29 Februry 2024; Received in revised form 11 March 2024; Accepted 15 March 2024
Available online 16 March 2024

Vishnu et al. [17] studied the addition of barium tungsten ($BaWO_4$) to natural rubber, which significantly improved the characteristics of gamma radiation shielding.

This search might encourage researchers to do experimental research on different kinds of metal tungstate oxides so that our results can be compared to those of future investigations. Researchers in technological fields who want to create novel chemicals for protecting themselves from radiation can benefit from this work. To accomplish this work, the desired metal tungstate oxides are $CaWO_4$ (CWO), $SrWO_4$ (SWO), $BaWO_4$ (BWO), and $PbWO_4$ (PWO) by theoretical investigation to examine their radiation attenuation properties.

2. Attenuation theory

2.1. Simulation procedures

A Monte Carlo simulation code (MCNP-5) input file is necessary for an adequate simulation procedure with an acceptable relative error value that can be used to estimate the average track length for various forms of ionizing radiation [18]. The shielding properties of the metal tungstate oxides were evaluated by instruction as displayed in **Fig. 1**. The elemental composition and the density of metal tungstate oxide samples are listed in **Table 1**. The input file consists of many cards, including surface, cell, material, importance, source, and physical cards. Regarding the surface card, it is used to describe the boundaries and dimensions of each cell. The cell is considered the smallest unit in geometry, where each consists of many cells arranged together. Besides, the material card is used to describe the chemical composition and density of each cell used in the geometry [2]. The F4 tally is used for detector to evaluation the average track length [19]. In addition, the results of simulation compared with theoretical values using the Phy-X/PSD software [20].

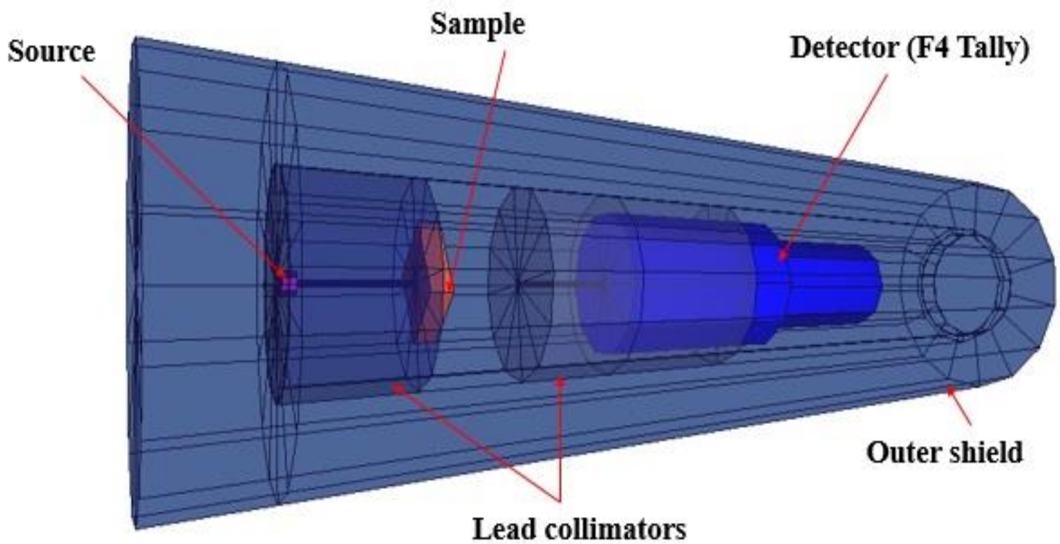

Fig.1. MCNP simulation geometry.

Table 1: The density, molar volume and elemental composition of metal tungsten oxides.

Metal tungstate oxides Code	Elements Fraction (wt. %)			Density (g/cm^3)	Molar Volume ($cm^3.mol^{-1}$)
	M	W	O		
CWO (M=Ca)	0.1392	0.6385	0.2223	6.10	47.202
SWO (M=Sr)	0.2612	0.5480	0.1908	6.31	53.163
BWO (M=Ba)	0.3565	0.4773	0.1662	6.25	61.626
PWO (M=Pb)	0.4553	0.4040	0.1406	7.96	57.166

2.2. Attenuation parameters calculation

To assess the gamma-ray absorption abilities, the current study used the gamma-ray attenuation equations for MWO_4 perovskite oxides (M = Ca, Sr, Ba, and Pb) as detailed below [21-25]. The narrow beam transport radiation setup could determine the attenuation coefficients for the studied shield material as follows:

$$I_x = I_0\, e^{-LAC\, x} \quad (1)$$

$$MAC = \left(\frac{LAC}{\rho}\right) = \frac{ln(\frac{I_0}{I_x})}{\rho x}, \quad (2)$$

Where; I_o and I_x are the without shield and attenuated intensities.

For theoretical computations, using the Phy-X/PSD software's program, the MFP, Z_{eff}, N_{eff}, HVL, and TVL values were obtained using measurements of LAC and MAC, which has been discussed in detail in references [2, 20].

3. Results and discussion

3.1. Radiation shielding parameters

Herein, the MWO_4 (M =Ca, Sr, Ba, and Pb) metal oxides capability to shield the gamma photons in the 0.081-1.408 MeV energy range using gamma sources (^{60}Co, ^{137}Cs, ^{133}Ba, and ^{152}Eu) was studied using the MCNP simulation code and Phy-X program 26. **Fig. 2** shows the LAC against gamma photon energy to adequately understand the shielding features of the metal tungstate oxides. **Table 2** depicts this comparison for the metal tungstate oxides with different compositions. Apparently, the MCNP and Phy-X values of the four metal tungstate oxides agreed highly with each other [26].

As the energy increases from 0.081 to 1.408 MeV, the LAC shows a decreasing pattern (**Fig. 2**). This decrease in LAC is brought on by radiation with relatively high energy since it penetrates the sample more readily. This indicates that the CWO, SWO, BWO, and PWO metal tungstate oxides possess the least (maximum) shield proficiency against high (lower) energy of radiation. The LAC values exhibit a tendency to rise as the MWO density of metal oxides rises, with the lowest (highest) value of 28.722 cm^{-1} (0.4229 cm^{-1}) at 0.081 MeV (1.408 MeV) for SWO and PWO, and the highest (lowest) value of 33.0154 cm^{-1} (0.3157 cm^{-1}) at 0.081 MeV (1.408 MeV) for PWO and BWO composite, respectively. The LAC increases with increasing atomic numbers from Ca, Sr, Ba, and Pb respectively, as does the density of metal tungstate oxides increases, as shown in **Table 1** [27, 28].

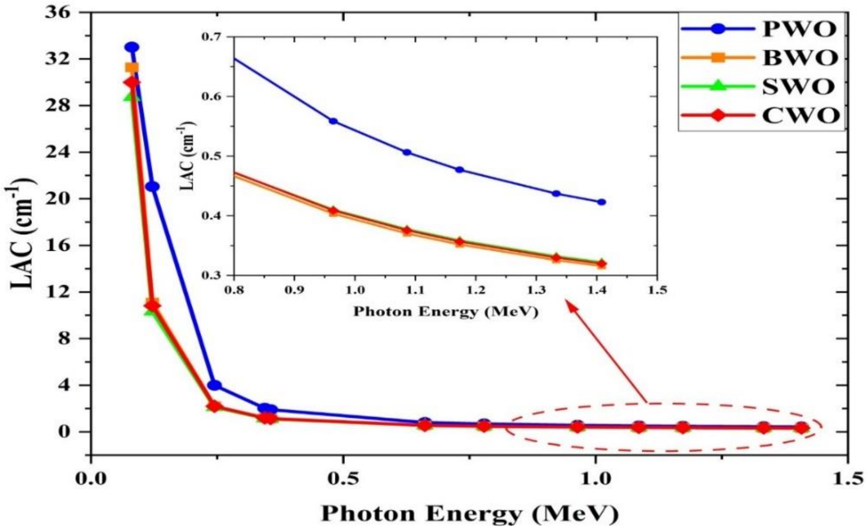

Fig. 2. Variation of the MWO_4 metal tungstate oxides LAC versus the gamma photon energy.

The metal tungstate oxide's mass attenuation coefficients are listed in **Table 2**, compared to values obtained from Phy-X calculations, which give a good agreement together. The MACs of the CWO, SWO, BWO, and PWO metal oxides were all compared at energies of ^{60}Co, ^{137}Cs, ^{133}Ba, and ^{152}Eu gamma ray sources to situate their protective the PWO abilities into perspective. When looking at the prepared metal tungstate oxides, BWO metal tungstate oxides have the greatest MAC, while CWO and SWO ceramics are practically slightly behind. The MAC values at 0.081 (1.408) MeV are equal to 4.917 (0.05245), 4.552 (0.05107), 5.006 (0.05052), and 4.148 (0.05313) cm^2/g for CWO, SWO, BWO, and PWO metal tungstate oxides, respectively, as shown in **Fig. 3**.

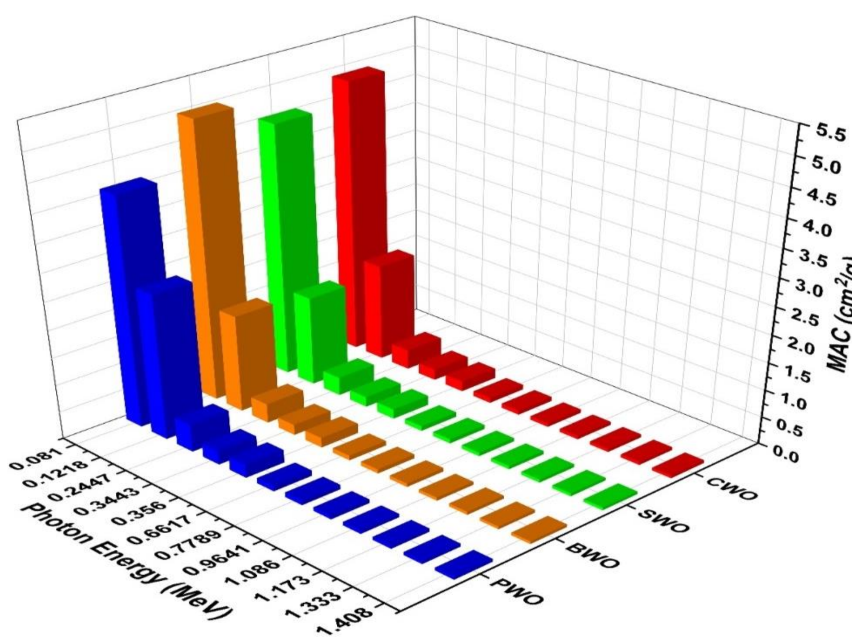

Fig. 3. The variation of MAC of MWO_4 metal-tungstate oxides versus the gamma photon energy.

Table 2: The MAC of metal-tungstate oxides.

Energy	$CaWO_4$			$SrWO_4$			$BaWO_4$			$PbWO_4$		
(MeV)	MCNP	Phy-x	RD%	MCNP	Phy-x	RD%	MCNP	Phy-x	RD%	MCNP	Phy-x	RD%
0.0810	4.91700	4.91694	0.0011	4.55200	4.55186	0.0030	5.00600	5.00544	0.0111	4.14800	4.14766	0.0082
0.1218	1.77400	1.77366	0.0192	1.63500	1.63492	0.0051	1.77400	1.77393	0.0037	2.64300	2.64342	0.0160
0.2447	0.35920	0.35924	0.0122	0.33420	0.33419	0.0025	0.35180	0.35177	0.0094	0.50150	0.50147	0.0065
0.3443	0.19630	0.19631	0.0040	0.18480	0.18477	0.0177	0.19070	0.19071	0.0051	0.25440	0.25443	0.0111
0.3560	0.18650	0.18651	0.0071	0.17580	0.17578	0.0121	0.18110	0.18109	0.0069	0.23980	0.23976	0.0157
0.6617	0.09047	0.09047	0.0022	0.08704	0.08704	0.0050	0.08721	0.08721	0.0010	0.10060	0.10056	0.0398
0.7789	0.07883	0.07883	0.0056	0.07612	0.07612	0.0043	0.07592	0.07592	0.0013	0.08509	0.08509	0.0056
0.9641	0.06707	0.06707	0.0028	0.06502	0.06502	0.0054	0.06457	0.06457	0.0029	0.07017	0.07017	0.0064
1.0860	0.06158	0.06160	0.0322	0.05980	0.05981	0.0221	0.05925	0.05927	0.0278	0.06358	0.06360	0.0328
1.1730	0.05851	0.05851	0.0030	0.05687	0.05687	0.0032	0.05630	0.05630	0.0085	0.05995	0.05995	0.0033
1.3330	0.05410	0.05410	0.0017	0.05265	0.05265	0.0000	0.05209	0.05209	0.0052	0.05492	0.05492	0.0044
1.4080	0.05245	0.05245	0.0017	0.05107	0.05107	0.0073	0.05052	0.05052	0.0069	0.05313	0.05313	0.0073

Fig. 4(a) shows the half-value layers (HVL) of the metal tungstate oxides as a function of gamma photon energy. HVL grows with energy; this clear trend indicates that in order to attenuate the same number of photons at higher energy, the graph also shows that, of the examined metal tungstate oxides, the PWO sample has a lower HVL than the MWO_4 samples, making them the more efficient barriers [29]. HVL values at 0.081 MeV (the minimum) and highest (1.408 MeV) gamma ray energy were equaled to 0.023 (2.166), 0.024 (2.151), 0.022 (2.195), and 0.021 (1.639) cm for CWO, SWO, BWO, and PWO metal tungstate oxides, respectively. Tenth-value layer (TVL) values are shown in **Fig. 4 (b)**. Herein, according to the TVL values at 0.081 MeV (lower) and highest (1.408 MeV) gamma ray energy, it was found to be 0.077 (7.197) cm, 0.080 (7.146) cm, 0.074 (7.293) cm, and 0.070 (5.445) cm for CWO, SWO, BWO, and PWO, respectively.

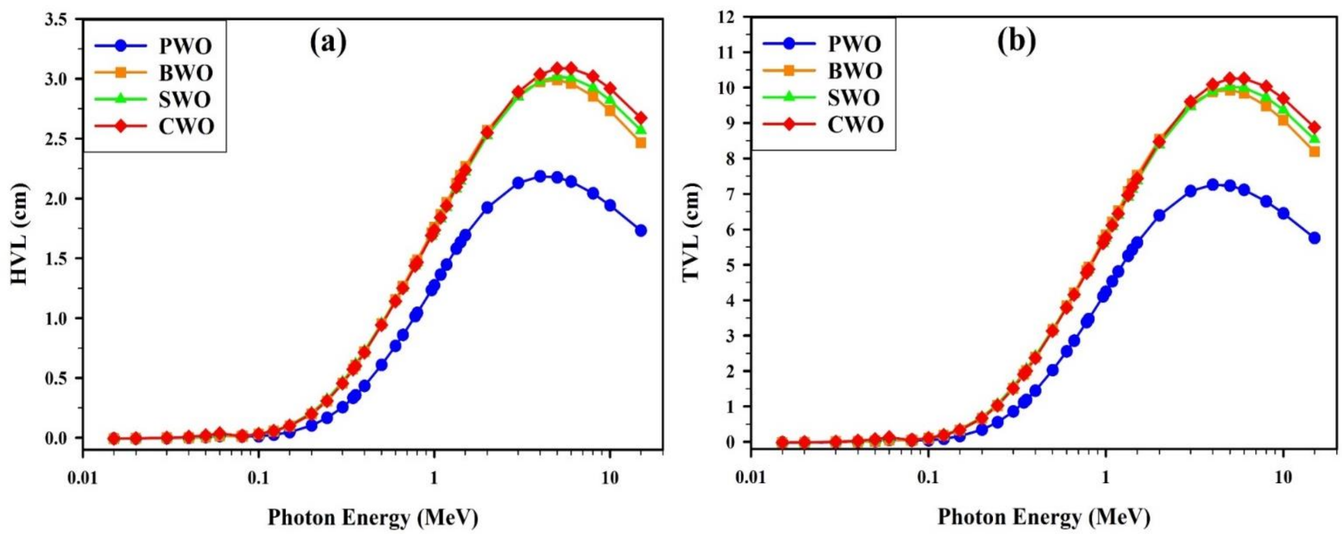

Fig. 4. Variation of the (a) HVL, (b) TVL for MWO_4 oxides versus the gamma photon energy.

The mean free path (MFP), another significant shield metric that is utilized to calculate the effective shield against ionizing radiation. In practical applications, it is preferred for metal tungstate oxides to have a lower MFP since it indicates greater photon contact with the material [30]. **Fig. 5** illustrates MFP results varying with investigated gamma source energies for the CWO, SWO, BWO, and PWO metal tungstate oxides. It was also revealed that the MFP energy dependent on the atomic number of metals added with WO_3 in the MWO_4 (M= Ca (z=20), Sr (z=38), Ba (z=56), and Pb (z=82)) metal tungstate oxides, as well as the density of the composite. The minimum MFP at PWO while the maximum MFP was reported at CWO ceramic. By contrast, the MFP at 0.662 MeV energy is 1.812, 1.821, 1.853, and 1.249 cm for CWO, SWO, BWO, and PWO metal tungstate oxides, respectively [31, 32].

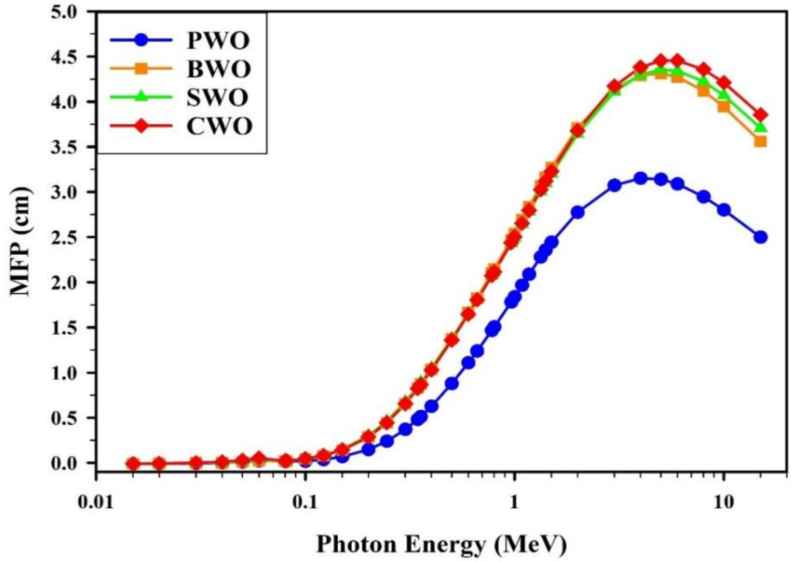

Fig. 5. Variation of MFP values for MWO_4 oxides versus the photon energies.

The effective atomic number (Z_{eff}) was also ascertained in order to understand the efficacy of the shielding material attenuation abilities. At high Z_{eff} values, the sample with the highest atomic number of heavy elements demonstrated a growing efficacy in attenuating gamma rays [33]. The Z_{eff} has relatively high values at first (< 0.8 MeV) with the PWO metal tungstate oxides with Pb concentrations having the largest and SWO having the lowest values. Following that, there is a significant decrease in Z_{eff} up to around 0.8 MeV. In the energy range of 0.8–1.4079 MeV, Z_{eff} achieves its lowest values, as seen in **Fig. 6(a)**. We observed that with higher energy (> 1 MeV) the PWO have large Z_{eff} values and CWO has the lowest. **Fig. 6(b)** demonstrates the variation of effective electron density (N_{eff}) with the photon energies. N_{eff} showed a commensurate response to the increase in metal at the MWO_4 composite, with a pattern that was similar to Z_{eff}'s.

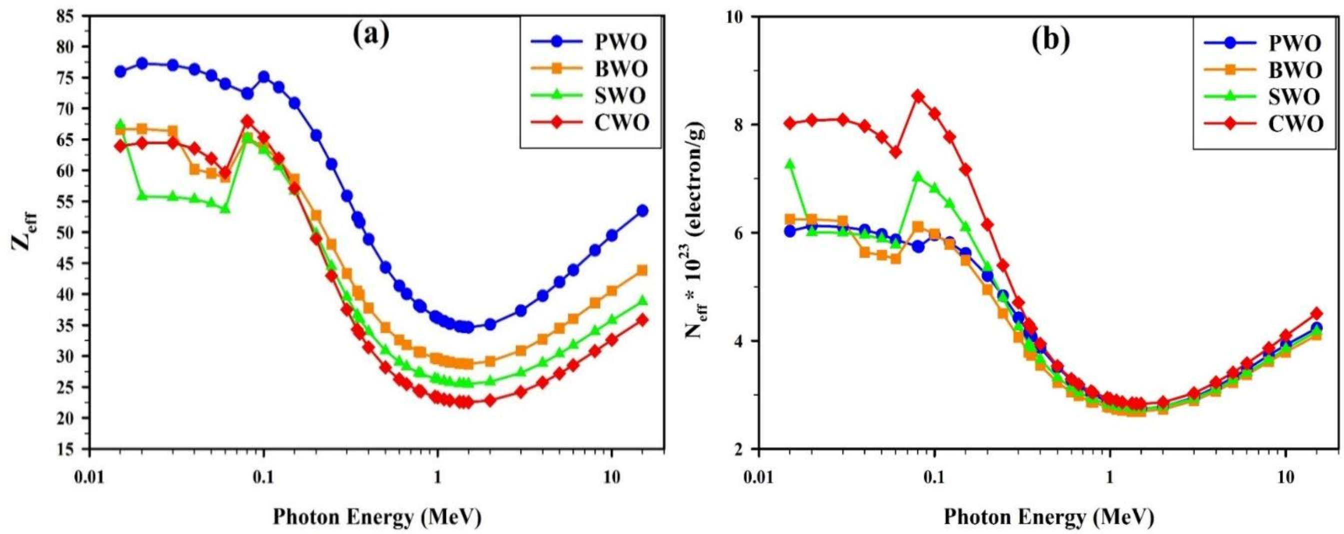

Fig. 6. Variations of the (a) Z_{eff} and (b) N_{eff} with photon energy for the MWO_4 metal tungstate oxides.

4. Conclusions

This work briefs the shielding features for metal tungstate oxides of MWO_4, where M =Ca, Fe, Sr, Ba, and Pb. The radiation protective parameters were examined using the MCNP code and Phy-X/PSD software in the gamma-ray energy range of 0.081-1.4079 MeV for gamma radiation sources ^{60}Co, ^{137}Cs, ^{133}Ba and ^{152}Eu. We also examined the LAC and MAC in the same energy range and observed a tendency for the attenuation ability to decrease from 0.81 to 1.4079 MeV. The LAC values exhibit a tendency to rise as the MWO density of metal oxides rises, with the lowest (highest) value of 28.722 cm^{-1} (0.4229 cm^{-1}) at 0.081 MeV (1.408 MeV) for SWO and PWO, and the highest (lowest) value of 33.0154 cm^{-1} (0.3157 cm^{-1}) at 0.081 MeV (1.408 MeV) for PWO and BWO composite, respectively. HVL values at 0.081 MeV (the minimum) and highest (1.408 MeV) gamma ray energy were equaled to 0.023 (2.166), 0.024 (2.151), 0.022 (2.195), and 0.021 (1.639) cm for CWO, SWO, BWO, and PWO metal tungstate oxides, respectively. The research results suggest that the correlation between the photon and the material depends upon the material's atomic density and composition of metal tungstate oxides. In addition, N_{eff} showed a commensurate response to the increase in metal at the MWO_4 composite, with a pattern that was similar to Z_{eff}'s. The results of this comparison study showed that the MWO_4 metal tungstate oxides could work well for radiation shielding applications.

Author Contributions

Said M. Kassem: Data curation, Investigation, Methodology, Writing - original draft, Writing - review & editing. Adel M. El Sayed: Data curation, Investigation, Writing - original draft. S. Ebraheem: Data curation, Supervision. A. I. Helal: Data curation, Supervision. Y. Y. Ebaid: Data curation, Supervision.

Declaration of Competing Interest

The authors declare that they have no known competing financial interests or personal relationships that could have appeared to influence the work reported in this paper.

References

[1] E. Hannachi, M. Sayyed, B. Albarzan, A.H. Almuqrin, K. Mahmoud, Synthesis and study of structural, optical and radiation-protective peculiarities of MTiO3 (M= Ba, Sr) metatitanate ceramics mixed with SnO_2 oxide, Ceramics International 47(20) (2021) 28528-28535.

[2] M. Sayyed, F.Q. Mohammed, K. Mahmoud, E. Lacomme, K.M. Kaky, M.U. Khandaker, M.R.I. Faruque, Evaluation of radiation shielding features of Co and Ni-based superalloys using MCNP-5 code: potential use in nuclear safety, Applied Sciences 10(21) (2020) 7680.

[3] E. Hannachi, M. Sayyed, K. Mahmoud, Y. Slimani, S. Akhtar, B. Albarzan, A.H. Almuqrin, Impact of tin oxide on the structural features and radiation shielding response of some ABO_3 perovskites ceramics (A= Ca, Sr, Ba; B= Ti), Applied Physics A 127(12) (2021) 970.

[4] E. Hannachi, K. Mahmoud, M. Sayyed, Y. Slimani, Structure, optical properties, and ionizing radiation shielding performance using Monte Carlo simulation for lead-free BTO perovskite ceramics doped with ZnO, SiO_2, and WO_3 oxides, Materials Science in Semiconductor Processing 145 (2022) 106629.

[5] Z.-X. Chen, Y. Chen, Y.-S. Jiang, Comparative study of ABO3 perovskite compounds. 1. ATiO3 (A= Ca, Sr, Ba, and Pb) perovskites, The Journal of Physical Chemistry B 106(39) (2002) 9986-9992.

[6] O. Sallam, M. Abdel Maksoud, S.M. Kassem, A. Awed, N. Elalaily, Enhanced linear and nonlinear optical properties of erbium/ytterbium lead phosphate glass by gamma irradiation for optoelectronics applications, Applied Physics A 128(9) (2022) 819.

[7] M.A. Maksoud, S.M. Kassem, O. Sallam, Structural, optical, and radiation shielding features of newly developed BaZrO3/Na2O–B2O3 glass, Ceramics International 48(20) (2022) 30938-30950.

[8] N.A. Saleh, M.Y. Alqahtani, M. Mhareb, F. Ercan, T. Ghrib, T.S. Kayed, B. Ozcelik, I. Ercan, F. ALbazzaz, R. Alanazi, Structural, magnetic and gamma-ray shielding features of cerium doped Mg2FeTiO6 double perovskite, Journal of Molecular Structure 1276 (2023) 134762.

[9] E. Hannachi, M. Sayyed, Y. Slimani, M. Almessiere, A. Baykal, M. Elsafi, Structure and radiation-shielding characteristics of BTO/MnZnFeO ceramic composites, Journal of Physics and Chemistry of Solids 174 (2023) 111132.

[10] E. Hannachi, M. Sayyed, K. Mahmoud, Y. Slimani, Gadolinium-based ceramics doped with lead oxide for γ-ray shielding, Materials Chemistry and Physics 291 (2022) 126731.

[11] S.B. Patel, A. Srivastava, R. Sharma, J.A. Abraham, V. Srivastava, Prediction of structural, electronic, mechanical, thermal, and thermoelectric properties in PbMO3 (M= Sb, Bi) perovskite compounds: a DFT study, The European Physical Journal Plus 137(3) (2022) 380.

[12] F. Akman, Z. Khattari, M. Kaçal, M. Sayyed, F. Afaneh, The radiation shielding features for some silicide, boride and oxide types ceramics, Radiation Physics and Chemistry 160 (2019) 9-14.

[13] M. Yılmaz, F. Akman, Gamma radiation shielding properties for polymer composites reinforced with bismuth tungstate in different proportions, Applied Radiation and Isotopes 200 (2023) 110994.

[14] E.E. Bayoumi, M.O. Abd El-Magied, E.A. Elshehy, B.M. Atia, K.A. Mahmoud, L.H. Khalil, A.A. Mohamed, Lead–bismuth tungstate composite as a protective barrier against gamma rays, Materials Chemistry and Physics 275 (2022) 125262.

[15] S.M. Kassem, M.A. Maksoud, M.M. Ghobashy, A.M. El Sayed, S. Ebraheem, A. Helal, Y. Ebaid, Novel flexible and lead-free gamma radiation shielding nanocomposites based on LDPE/SBR blend and BaWO4/B2O3 heterostructures, Radiation Physics and Chemistry 209 (2023) 110953.

[16] E. Hannachi, Y. Slimani, M. Sayyed, K. Mahmoud, Scheelite-type BaWO4 doped with Ho2O3 oxide as a promising lead-free shield for gamma rays: Structural, optical properties, and radiation attenuation efficiency, Materials Science in Semiconductor Processing 167 (2023) 107802.

[17] C. Vishnu, A. Joseph, Gamma-ray shielding analysis on natural rubber composites fortified with barium tungstate (BaWO4), Radiation Physics and Chemistry 216 (2024) 111389.

[18] E. Hannachi, Y. Slimani, M. Sayyed, K. Mahmoud, Synthesis of lead oxide doped SmBa2Cu3Oy ceramic systems as efficient shields against γ radiations: Structure, radiation attenuating capacities, and optical features, Ceramics International 48(21) (2022) 31902-31908.

[19] G. Lakshminarayana, I. Kebaili, M. Dong, M.S. Al-Buriahi, A. Dahshan, I.V. Kityk, D.-E. Lee, J. Yoon, T. Park, Estimation of gamma-rays, and fast and the thermal neutrons attenuation characteristics for bismuth tellurite and bismuth boro-tellurite glass systems, Journal of materials science 55 (2020) 5750-5771.

[20] E. Şakar, Ö.F. Özpolat, B. Alım, M. Sayyed, M. Kurudirek, Phy-X/PSD: development of a user friendly online software for calculation of parameters relevant to radiation shielding and dosimetry, Radiation Physics and Chemistry 166 (2020) 108496.

[21] Y. Yan, H. Yang, Z. Yi, R. Li, T. Xian, Design of ternary CaTiO3/g-C3N4/AgBr Z-scheme heterostructured photocatalysts and their application for dye photodegradation, Solid State Sciences 100 (2020) 106102.

[22] Y. Slimani, B. Unal, M.A. Almessiere, E. Hannachi, G. Yasin, A. Baykal, I. Ercan, Role of WO3 nanoparticles in electrical and dielectric properties of BaTiO3–SrTiO3 ceramics, Journal of Materials Science: Materials in Electronics 31(10) (2020) 7786-7797.

[23] Y. Slimani, A. Selmi, E. Hannachi, M.A. Almessiere, M. Mumtaz, A. Baykal, I. Ercan, Study of tungsten oxide effect on the performance of BaTiO 3 ceramics, Journal of Materials Science: Materials in Electronics 30 (2019) 13509-13518.

[24] S.R. Srither, N.R. Dhineshbabu, Synthesis and characterisation of FeTiO3 perovskite nanomaterials for electrochemical energy storage application, Micro & Nano Letters 14(5) (2019) 475-478.

[25] A. Sobhani-Nasab, M. Rangraz-Jeddy, A. Avanes, M. Salavati-Niasari, Novel sol–gel method for synthesis of PbTiO 3 and its light harvesting applications, Journal of Materials Science: Materials in Electronics 26 (2015) 9552-9560.

[26] Y. Slimani, M.K. Hamad, I. Olarinoye, Y. Alajerami, M. Sayyed, M. Almessiere, M. Mhareb, Determination of structural features of different Perovskite ceramics and investigation of ionizing radiation shielding properties, Journal of Materials Science: Materials in Electronics 32 (2021) 20867-20881.

[27] M. Abdel Maksoud, O. Sallam, S.M. Kassem, R.A. Fahim, A. Awed, Novel strategy for hazardous cement bypass dust removal: Structural, optical and nuclear radiation shielding properties of CBD-bismuth borate glass, Journal of Inorganic and Organometallic Polymers and Materials 32(9) (2022) 3533-3545.

[28] M. Sayyed, E. Hannachi, K. Mahmoud, Y. Slimani, Synthesis of different (RE) BaCuO ceramics, study their structural properties, and tracking their radiation protection efficiency using Monte Carlo simulation, Materials Chemistry and Physics 276 (2022) 125412.

[29] A.H. Almuqrin, M. Sayyed, S. Hashim, A. Kumar, Exploring the impact of PbO/CdO composition on the structural, optical, and gamma ray shielding properties of dense PbO–TeO2–CdO glasses, Optical Materials 138 (2023) 113698.

[30] M. Abdel Maksoud, E. Abou Hussein, S.M. Kassem, R.A. Fahim, A. Awed, Effect of CeO2 addition on structural, optical, and radiation shielding properties of B2O3–Na2O–SrO glass system, Journal of Materials Science: Materials in Electronics 32(14) (2021) 18931-18950.

[31] M. Alqahtani, F. Ercan, N.A. Saleh, M. Mhareb, N. Dwaikat, M. Sayyed, F. Abokhamis, A. Abdulrazzaq, B. Özcelik, I. Ercan, Structural, magnetic and gamma-ray shielding features of Zn doped Mg2FeTiO6 double perovskite, Physica B: Condensed Matter 640 (2022) 414024.

[32] E. Hannachi, M. Sayyed, Y. Slimani, M. Elsafi, Structural, optical and radiation shielding peculiarities of strontium titanate ceramics mixed with tungsten nanowires: An experimental study, Optical Materials 135 (2023) 113317.

[33] K. Mahmoud, O. Tashlykov, M. Sayyed, E. Kavaz, The role of cadmium oxides in the enhancement of radiation shielding capacities for alkali borate glasses, Ceramics International 46(15) (2020) 23337-23346.